Interpretation of Biphasic Dissociation Kinetics for Isomeric Class II Major Histocompatibility Complex-Peptide Complexes

Thomas G. Anderson and Harden M. McConnell*
Department of Chemistry, Stanford University, Stanford, California 94305 USA

ABSTRACT Antigenic peptides bound to class II major histocompatibility complex (MHC) proteins play a key role in the distinction between "self" and "nonself" by the cellular immune system. Although the formation and dissociation of these complexes are often thought of in terms of the simple mechanism MHC + P $\rightleftharpoons$ MHC-P, studies of MHC-peptide dissociation kinetics suggest that multiple interconverting forms of the bound MHC-peptide complex can be formed. However, the precise relationship between observed dissociation data and proposed multiple-complex mechanisms has not been systematically examined. Here we provide a mathematical analysis to fill this gap and attempt to clarify the kinetic behavior that is expected to result from the proposed mechanisms. We also examine multiple-complex dynamics that can be "hidden" in conventional experiments. Although we focus on MHC-peptide interactions, the analysis provided here is fully general and applies to any ligand-receptor system having two distinct bound states.

INTRODUCTION

Proteins of the class II major histocompatibility complex (MHC) are expressed on the surface of antigen-presenting cells, where they display peptide fragments to receptors on $CD4^+$ T helper cells. Like antibodies, these T-cell receptors (TCRs) exhibit great diversity at their recognition site (Davis and Bjorkman, 1988; Davis, 1990; Garboczi et al., 1996; Garcia et al., 1996; Jardetzky, 1997), enabling them to distinguish between different peptides in the context of the MHC protein, effecting the specific cellular immune response (reviewed in Abbas et al., 1994). It is generally assumed that the immunologically active form of an MHC-peptide complex adopts a single unique structure that can be recognized by the TCR. However, a growing body of evidence suggests that multiple isomeric complexes can be formed in MHC-peptide systems (Dornmair et al., 1989; Sadegh-Nasseri and McConnell, 1989; Beeson and McConnell, 1994; Beeson et al., 1996; Schmitt et al., 1998a,b). In several cases, these isomeric complexes can be distinguished by T cells (Viner et al., 1996; Rabinowitz et al., 1997).

The structural changes involved in the formation of isomeric complexes are not well understood. Although the static structures of several MHC-peptide complexes from mice as well as humans have been characterized by x-ray crystallography (Brown et al., 1993; Fremont et al., 1996, 1998; Jardetzky et al., 1996; Scott et al., 1998), such structures provide little information about the dynamics of the complexes. Rather than rely upon structural data alone, this laboratory has investigated MHC-peptide isomers indirectly by studying the kinetics of formation and dissociation of MHC-peptide complexes. Kinetic experiments have been instrumental in elucidating the mechanism of MHC-peptide binding (Fig. 1 *A*), which is thought to involve numerous reactions. Initially present complexes of MHC with endogenous peptides (MP_e) can dissociate to form empty MHC (M) (Witt and McConnell, 1991, 1992). This "active" unbound MHC can reversibly convert to a "dormant" form (M_I) (Rabinowitz et al., 1998; Natarajan et al., 1999) or be irreversibly inactivated (forming M_X) (Mason and McConnell, 1994). We shall not discuss these steps in detail here. In studies of binding to labeled peptides (P*), it has been shown in several cases that MHC can form multiple isomeric complexes ($\{MP^*\}_1$ and $\{MP^*\}_2$) (Sadegh-Nasseri and McConnell, 1989; Witt and McConnell, 1992; Sadegh-Nasseri et al., 1994). Reactions of these complexes, particularly interconversion and dissociation, will be the focus of our discussion. Additional reactions not shown in Fig. 1 have also been proposed, for example, the displacement of one peptide by another via a transient two-peptide intermediate (Tampé and McConnell, 1991; de Kroon and McConnell, 1993, 1994; Witt and McConnell, 1994). We will not discuss these ancillary reactions further, restricting our discussion to the subset of reactions shown in Fig. 1 *B*.

To assess the biological significance of isomeric MHC-peptide complexes, it is important to know how and under what conditions the different isomers are formed. If one isomer is formed in vanishingly small amounts, or if the two complexes interconvert very rapidly, the complexes might not be distinguished by T cells. However, if isomeric MHC-peptide complexes interconvert slowly, they might give rise to distinct immune responses because of the short (~10 s) duration of MHC-peptide/TCR interactions under physiological conditions (Matsui et al., 1991, 1994). This could be particularly important if different MHC-peptide isomers are preferentially formed in different in vivo environments. To address these issues, it is necessary to solve the biophysical problem of determining the proportions of the isomeric

Received for publication 16 December 1998 and in final form 2 August 1999.

Address reprint requests to Dr. Harden M. McConnell, Department of Chemistry, Stanford University, Stanford, CA 94305-5080. Tel.: 650-723-4571; Fax: 650-723-4943; E-mail: harden@leland.stanford.edu.

0006-3495/99/11/2451/11 $2.00

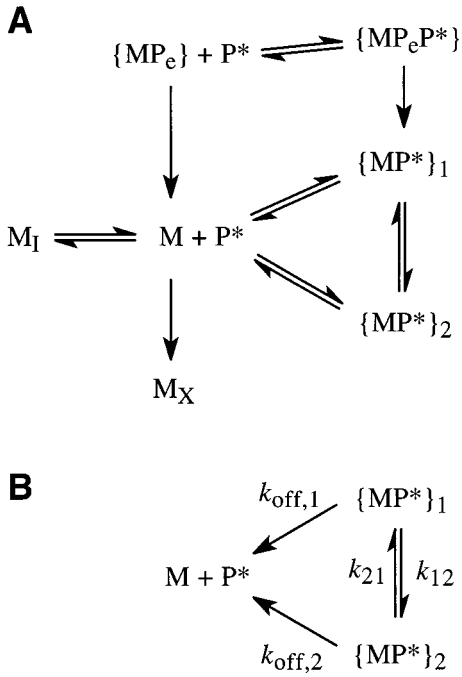

FIGURE 1 Dynamics of the peptide-MHC system. (*A*) Reactions that have been inferred from kinetics experiments to occur in MHC-peptide interaction. The species involved are M, "active" unbound MHC; P*, labeled peptide; M_I, "dormant" inactive MHC; M_X, permanently inactivated MHC; $\{MP_e\}$, MHC bound to endogenous peptide; $\{MP^*P_e\}$, ternary complex of labeled and endogenous peptides with MHC; $\{MP^*\}_1$ and $\{MP^*\}_2$, isomeric forms of the labeled peptide-MHC complex. (*B*) The subset of reactions involved in the dissociation of the MHC-peptide complexes.

complexes that are present under various conditions, as well as the rates at which they form and interconvert.

Unfortunately, the MHC-peptide system presents a number of obstacles to conventional kinetic analysis. Side reactions of the empty MHC molecule and formation of empty MHC by the dissociation of prebound endogenous peptides make it difficult to interpret measurements of the binding rates and equilibrium binding constants of labeled peptides. Consequently, in the analysis presented here we restrict our discussion to MHC-peptide dissociation reactions (Fig. 1 *B*). Although multiple forms of peptide-MHC complexes are known (Boniface et al., 1996; Dadaglio et al., 1997; Runnels et al., 1996), isomeric complexes of the labeled MHC-peptide complex are not directly observed in kinetic experiments, so the relative concentrations of these complexes are generally unknown. The absence of well-defined initial conditions greatly complicates the analysis of kinetic data from MHC-peptide reactions (Steinfeld et al., 1989).

The relationships between the observed dissociation rate constants and the microscopic rate constants are complicated for all but the simplest cases. To illustrate our analysis of MHC-peptide dissociation kinetics, we shall discuss kinetic data for a simulated two-complex MHC-peptide system with arbitrarily chosen microscopic rate constants. In addition, we will briefly apply the analysis to previously published kinetic experiments to demonstrate the application of this analysis to real experimental data. Although we present our discussion in terms of MHC-peptide interactions, the analysis provided here is fully general and applies to dissociation studies of any ligand-receptor system having two kinetically distinct bound states.

EXPERIMENTAL TECHNIQUES

Preparation and dissociation of MHC-peptide complexes

The preparation of MHC-peptide complexes involves incubating MHC proteins with an excess of peptide that is labeled with a radioactive tag (Sadegh-Nasseri et al., 1994), a fluorescent moiety (Tampé and McConnell, 1991; Witt and McConnell, 1994), or some other detectable group (Jensen, 1992). This incubation is typically carried out under quasiphysiological conditions of pH 5.3, 150 mM sodium chloride, and 37°C, to mimic the conditions under which MHC loading occurs within the endosomal compartments of antigen-presenting cells (Tulp et al., 1994). After a period of incubation, which generally lasts 10–20 h, the complex formed is separated from unbound peptide, using a size exclusion column (Witt and McConnell, 1991; de Kroon and McConnell, 1993). Samples of the incubation mixture may be taken at various time points during the course of the binding reaction; the amount of labeled peptide bound to the MHC can then be measured to provide a profile of the binding kinetics (Witt and McConnell, 1991; de Kroon and McConnell, 1993; Liang et al., 1995).

In a dissociation experiment, labeled MHC-peptide complex is prepared and isolated as described above. The complex is then incubated under the dissociation conditions of interest, which may or may not be the same as the binding conditions. The amount of labeled complex is then measured over time as the labeled peptide dissociates from the MHC. An unlabeled competitor peptide is sometimes added to the incubation to inhibit rebinding of dissociated peptide. The collected data are normalized and fit to either a mono- or biexponential decay curve (Witt and McConnell, 1994), as illustrated by Eqs. 1 and 2:

$$\frac{[\{MP^*\}](t)}{[\{MP^*\}]_0} = e^{-k^o_{off}t} \tag{1}$$

$$\frac{[\{MP^*\}](t)}{[\{MP^*\}]_0} = F^o e^{-k^o_{fast}t} + S^o e^{-k^o_{slow}t} \tag{2}$$

The superscript o indicates the observed kinetic parameters. For the biphasic curve, the magnitudes of the fast and slow exponential phases are denoted by F^o and S^o, respectively. For the biphasic dissociation curve, $F^o + S^o = 1$. Such a dissociation curve is shown in Fig. 2.

Numerical simulations of experimental data

Dissociation curves and other experimental data for the hypothetical MHC-peptide system discussed in this paper were generated by the numerical evaluation of rate equations. Differential equations describing the rates of reaction for the species shown in Fig. 1 *A* were integrated numerically using *Mathematica* 3.0 (Wolfram Research) to determine the concentrations of the species as functions of time. Magnitudes of the fast and slow exponential phases of dissociation were taken from fits of the biexponential equation (Eq. 2) to the simulated dissociation data. Except as otherwise noted, values for the rate constants and initial concentrations were taken from previous kinetic simulations (Beeson et al., 1996; Rabinowitz et al., 1998). Rate constants: dissociation of endogenous peptide, $k_e = 2\ h^{-1}$; reversible inactivation of MHC, $k_{ai} = 15\ h^{-1}$; activation of dormant MHC, $k_{ia} = 0.25\ h^{-1}$; irreversible inactivation of MHC, $k_x = 0.05\ h^{-1}$; formation of $\{MP^*\}_1$, $k_{on,1} = 360\ \mu M^{-1}\ h^{-1}$; dissociation of $\{MP^*\}_1$, $k_{off,1} = 0.7\ h^{-1}$; conversion of $\{MP^*\}_1$ to $\{MP^*\}_2$, $k_{12} = 0.48\ h^{-1}$; conversion of

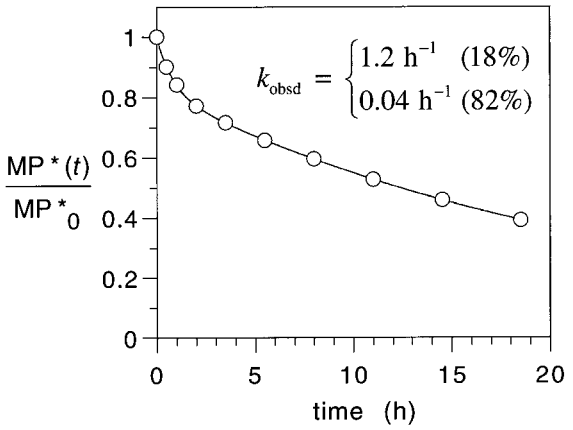

FIGURE 2 A typical biphasic dissociation curve for the simulated MHC-peptide system discussed in the text. The time dependence of the total concentration of complex is fit by $[\{MP^*\}]/[\{MP^*\}]_0 = 0.18e^{-1.2t} + 0.82e^{-0.04t}$. The observed parameters are the magnitude of fast phase, $F^o = 0.18$; the rate constant of the fast phase, $k^o_{fast} = 1.2\ h^{-1}$; and the rate constant of the slow phase, $k^o_{slow} = 0.04\ h^{-1}$.

$\{MP^*\}_2$ to $\{MP^*\}_1$, $k_{21} = 0.048\ h^{-1}$; formation of $\{MP^*\}_2$, $k_{on,2} = 61.7\ \mu M^{-1}\ h^{-1}$; dissociation of $\{MP^*\}_2$, $k_{off,2} = 0.012\ h^{-1}$. Initial concentrations used for simulation of binding reactions: endogenous complex, $[\{MP_e\}]_0 = 1\ \mu M$; all other MHC species = 0; labeled peptide, $[P^*]_0 = 100\ \mu M$. For dissociation reactions, the initial concentration of labeled peptide was set at zero, and the initial concentration of unlabeled competitor peptide was set at 100 μM.

RESULTS AND DISCUSSION

Ambiguous dissociation kinetics

Fig. 2 shows a simulated dissociation curve for a complex of MHC with peptide P*. The distinct biexponential shape of the curve is not consistent with the simple reaction MP* $\rightarrow$ M + P*. Two distinct MHC-peptide complexes must be involved in the dissociation, as illustrated by Fig. 1 *B* (Sadegh-Nasseri and McConnell, 1989). If the two complexes were distinguishable by spectroscopic or other means, their individual concentrations could be measured over time to provide a complete picture of the kinetics of the system (Fig. 3). However, for kinetic studies of MHC-peptide systems, isomeric complexes of the MHC-peptide complex generally appear as a single signal (see Experimental Techniques), providing no information about the individual concentrations of the complexes. As a consequence, many different MHC-peptide systems with disparate microscopic behaviors could give rise to the same observed dissociation curve (Fig. 3).

There are four microscopic rate constants involved in the dissociation of a two-complex MHC-peptide system (Fig. 1 *B*), yet there are only two macroscopic rate constants observed (Fig. 2). Without concentration data, there are two degrees of freedom in the "solution space" of systems that are consistent with our observed dissociation curve (Fig. 4). We want to determine where our system lies in this solution space. That is, we wish to know the microscopic kinetic

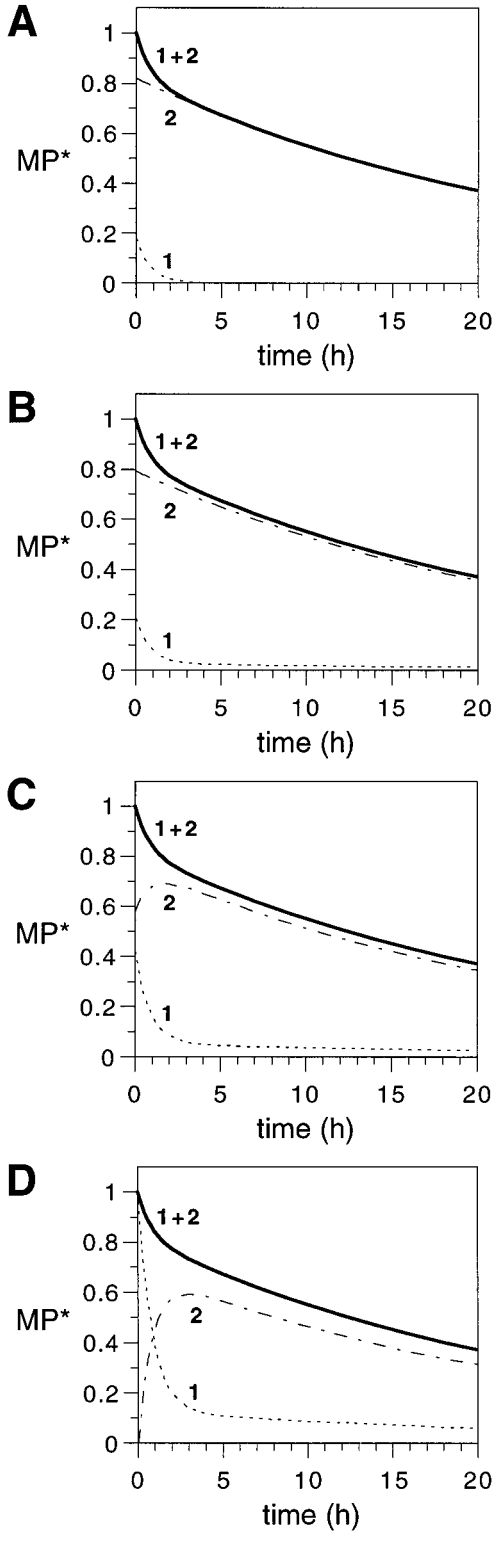

FIGURE 3 Many different two-complex MHC-peptides produce the observed dissociation curve shown in Fig. 2. Shown are dissociation curves for (*A*) Scheme 1, (*B*) Scheme 2, (*C*) Scheme 3, and (*D*) Scheme 4, discussed in the text. The behavior of Scheme 5 is very similar to that of *B*. Dashed lines indicate the concentrations of complexes $\{MP^*\}_1$ (– – –) and $\{MP^*\}_2$ (— - —); the total concentration of complex is indicated by the solid line. Note that although the behavior of the individual complexes differs from one reaction scheme to another, the observed total concentration is identical for all of them.

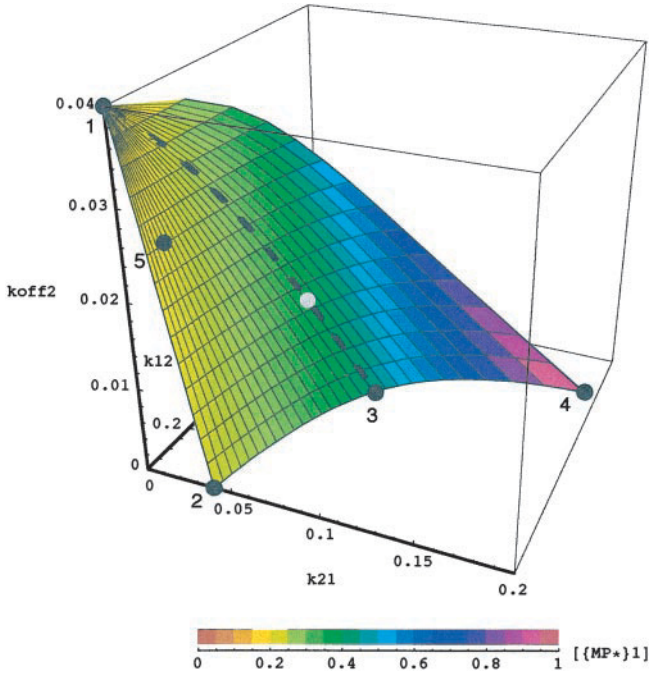

FIGURE 4 The set of systems that produce the dissociation curve shown in Fig. 2 lies on a two-dimensional surface in "kinetic space." The three axes correspond to the values of the microscopic rate constants k_{12}, k_{21}, and $k_{off,2}$; the fourth microscopic rate constant, $k_{off,1}$, is related to the others by Eq. 20 (Table 1). The fraction of complex in the form $\{MP^*\}_1$ is indicated by color. Each point on the surface shown represents an MHC-peptide system that produces the observed dissociation curve; the points corresponding to Schemes 1–5 are indicated. The dotted line indicates the subset of this solution space, which is also consistent with the data shown in Fig. 4. The gray dot indicates the system that was used to numerically simulate the data in Figs. 2 and 4.

parameters (rate constants and initial concentrations) of the system that produced the dissociation curve shown in Fig. 2. Before addressing this issue, we shall first examine several "candidate" systems that are consistent with these dissociation data.

The parallel system

One candidate is the "parallel" system, with two noninterconverting complexes with the dissociation rate constants and initial populations shown in Scheme 1.

$$\begin{array}{ccc} (18\%) & \overset{\sim 0}{\rightleftharpoons} & (82\%) \\ \{MP^*\}_1 & \underset{\sim 0}{} & \{MP^*\}_2 \\ 1.2\ h^{-1}\searrow & & \swarrow 0.04\ h^{-1} \\ & M + P^* & \end{array}$$

Scheme 1

As shown, the rate of interconversion between the complexes in this system is negligible. This system produces the dissociation curve shown in Fig. 2. Interpreting the dissociation kinetics according to this scheme, the observed fast and slow exponential phases of the dissociation curve correspond to the dissociation of complexes $\{MP^*\}_1$ and $\{MP^*\}_2$, respectively. The microscopic observed rate constants $k_{off,1}$ and $k_{off,2}$ are equal to k^o_{fast} and k^o_{slow}, and the amplitudes of the fast and slow exponential phases in the dissociation curve faithfully reflect the initial populations of the two complexes. This is the simplest interpretation of the observed dissociation data.

Sequential systems

The parallel system is not the only solution consistent with our data, however. One could also account for the observed dissociation curve with a "sequential" system in which the two complexes can slowly interconvert, as shown in Scheme 2.

$$\begin{array}{ccc} (21\%) & \overset{\ll 0.04\ h^{-1}}{\rightleftharpoons} & (79\%) \\ \{MP^*\}_1 & \underset{0.04\ h^{-1}}{} & \{MP^*\}_2 \\ 1.2\ h^{-1}\searrow & & \swarrow \sim 0 \\ & M + P^* & \end{array}$$

Scheme 2

Here, complex $\{MP^*\}_2$ does not dissociate directly at an appreciable rate. Rather, it dissociates through the "kinetic intermediate" $\{MP^*\}_1$. The initial populations of the two complexes are still close to the magnitudes of the observed fast and slow dissociation phases, and the microscopic rate constants $k_{off,1}$ and k_{21} are equal to the observed rate constants k^o_{fast} and k^o_{slow}. Scheme 2 also produces the observed dissociation curve shown in Fig. 2.

Other schemes that are consistent with the observed dissociation curve can be proposed in which the interconversion of the complexes is more rapid. In such systems, the observed kinetics are distorted from the microscopic rates. For example, the system shown in Scheme 3 produces the MP* dissociation curve in Fig. 2, even though the microscopic rate constants do not match the observed rate constants and the initial populations of the two complexes are far from the magnitudes of the observed fast and slow dissociation phases.

$$\begin{array}{ccc} (42\%) & \overset{0.56\ h^{-1}}{\rightleftharpoons} & (58\%) \\ \{MP^*\}_1 & \underset{0.08\ h^{-1}}{} & \{MP^*\}_2 \\ 0.60\ h^{-1}\searrow & & \swarrow \sim 0 \\ & M + P^* & \end{array}$$

Scheme 3

The kinetic distortions seen in this sequential scheme can be understood in terms of a steady-state approximation for the fast-dissociating complex $\{MP^*\}_1$. In the fast phase of dissociation, the population of $\{MP^*\}_1$ rapidly drops to its steady-state level, with a rate constant k^o_{fast} about equal to $k_{off,1} + k_{12} = 0.60\ h^{-1} + 0.56\ h^{-1} = 1.16\ h^{-1}$. After $\{MP^*\}_1$ reaches this level, the steady-state approximation tells us that the system decays with a rate constant k^o_{slow} of $(k_{21}\ k_{off,1})/(k_{off,1} + k_{12}) = 0.041\ h^{-1}$. These are the values of k^o_{fast} and k^o_{slow} that are observed in Fig. 2. The steady-state

approximation also helps rationalize the observed magnitude of the fast dissociation phase. Because the initial population of fast-dissociating $\{MP^*\}_1$ is partitioned over dissociation and interconversion reactions, the initial 42% population of $\{MP^*\}_1$ gives rise to only an 18% observed fast phase. It should be recognized that the steady-state approximation is not a precise treatment of this reaction scheme. A more detailed analysis, provided in the Appendix and summarized in Table 1, shows that the relationship between the observed kinetics and the microscopic rate constants is in fact much more complicated.

Kinetic partitioning distorts the rate constants and populations in any MHC-peptide system for which the rate of conversion of $\{MP^*\}_1$ to $\{MP^*\}_2$ is comparable to the other reaction rates. This means that, except in the case of the parallel system, the magnitude of the observed fast phase in a dissociation reaction *underestimates* the initial population of the complex $\{MP^*\}_1$, sometimes to a great degree. Consider the system shown in Scheme 4, which is also consistent with the dissociation curve in Fig. 2.

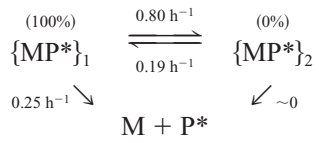

Scheme 4

In this case, *all* of the complex is initially present in the faster-dissociating form $\{MP^*\}_1$, yet the magnitude of the observed fast dissociation phase is only 18%.

Complete mechanisms

In the examples discussed so far, one or more microscopic reaction rates are negligible. However, most of the solution space for our dissociation curve consists of reaction systems in which all of the microscopic reactions proceed at significant rates. One example of such a system is shown in Scheme 5; like the other examples, it too generates the biphasic dissociation curve in Fig. 2.

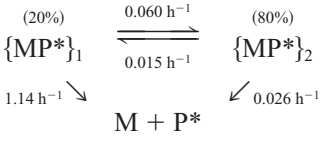

Scheme 5

This particular example is interesting because the two complexes are initially at equilibrium: the ratio of the initial concentrations of $\{MP^*\}_2$ to $\{MP^*\}_1$ is equal to $K_{1\rightleftharpoons 2} = k_{12}/k_{21} = 4$.

Although there is a diverse range of systems that are consistent with our observed dissociation curve, we can place limits on the values of the microscopic parameters of the actual MHC-peptide system. As shown in Fig. 4, the microscopic rate constant $k_{off,1}$ must be less than or equal to the observed k^o_{fast} (1.2 h^{-1}), and $k_{off,2}$ must be less than or equal to k^o_{slow} (0.04 h^{-1}). The rate constants for interconversion, k_{12} and k_{21}, can range from 0 (in the case of the parallel scheme) to a value less than the observed k^o_{fast}. The fraction of complex initially in the form $\{MP^*\}_1$ must be greater than F^o, the observed magnitude of the fast dissociation phase, and can, in principle, be as high as 100%.

For simplicity, the observed magnitudes (F^o and S^o) and rate constants (k^o_{fast} and k^o_{slow}) of biphasic MHC-peptide dissociation curves in previous reports have often been taken as readouts of the initial concentrations and dissociation rate constants of the faster and slower dissociating complexes (Beeson and McConnell, 1994; Beeson et al., 1996; Rabinowitz et al., 1997). However, as the above examples demonstrate, this simple interpretation is valid only if the complexes interconvert very slowly relative to the dissociation reactions. Slow interconversion need not be the case, however. Experiments involving "regeneration" of a fast dissociation phase from partially dissociated MHC-peptide complexes show that the interconversion rate of isomeric complexes can be comparable to or faster than that of dissociation reactions (Schmitt et al., 1998b). In the absence of additional information, therefore, it is generally prudent to consider the full range of consistent systems when interpreting MHC-peptide dissociation kinetics.

Information from variation of binding time

Although it is generally not possible to determine the initial concentrations of the two isomeric complexes in a typical dissociation experiment, one can nevertheless manipulate these concentrations to some extent by varying the length of the binding incubation that precedes the dissociation. Because the two MHC-peptide complexes are almost certainly formed at different rates, the relative populations of the complexes should depend on the length of the binding incubation. Therefore, by changing the binding time, one can systematically vary the ratio of the complexes' concentrations for different dissociation experiments. This variation in concentrations shows up indirectly in the observed magnitude of fast dissociation phase, F^o, over a range of binding incubation times (Fig. 5).

Measurement of the magnitude of fast dissociation phase after different binding times provides additional information about the microscopic kinetics of the system. Fig. 5 *A* shows a plot of the observed magnitude of fast dissociation phase, F^o, for simulated dissociations after binding incubations of up to 20 h; this curve is an approximately exponential decay from a maximum of $F^o_0 = 0.48$ at zero binding time, with a limiting value of 0.03 at long binding times. The data can also be plotted as the ratio of the observed slow and fast dissociation phases, producing the sigmoidal curve shown in Fig. 5 *B*. The precise shapes of these curves depend upon the rate of complex formation, which is limited by the rate at which MHC becomes available for binding the labeled peptide through dissociation of endogenous peptide or by

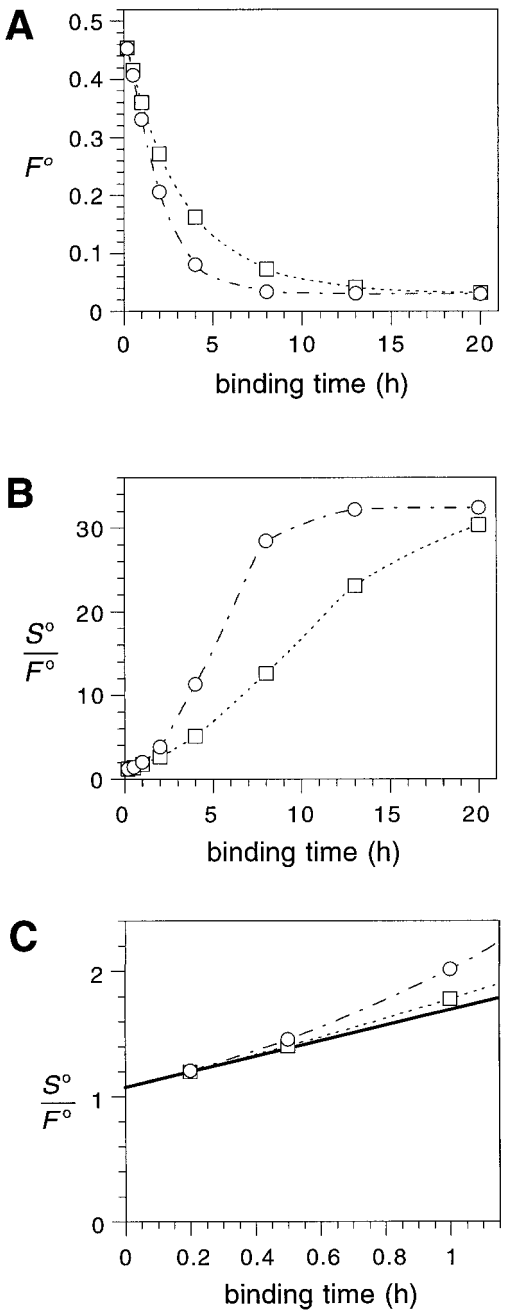

FIGURE 5 The magnitude of observed fast phase, F^o, after binding incubations of 0.2, 0.5, 1, 2, 4, 8, 13, and 20 h for two simulations of a two-complex reaction system with the same observed dissociation rate constants as in Fig. 2. The simulations used the rate constants given in Experimental Techniques, with an initial peptide concentration of 100 μM and 1 μM MHC protein initially in the form $\{MP_e\}$ (○) or M_I (□). (*A*) The value of F^o is greatest after short binding incubations and decreases for longer binding incubations. (*B*) The ratio of the observed slow and fast dissociation phases as a function of binding time. Note that the precise shapes of these curves depend upon reactions that precede complex formation, but the values extrapolated to binding times of 0 and infinity (1.074 and 32.4) are in the same ratio as the observed rate constants (k^o_{fast}/k^o_{slow} = 30) and are independent of the binding process. (*C*) A close-up of the curve from *B*, showing the ratio of the slow to the fast dissociation phase after short incubation times for the two simulations. The solid line illustrates the limiting value of the slope of this curve, as calculated from the kinetic model. The S^o/F^o ratio extrapolated to zero binding time is 1.074, corresponding to a magnitude of the fast phase $F^o_0 = 0.482$.

activation of "dormant" empty MHC (Rabinowitz et al., 1998). However, the limits of the curves in zero and infinite binding time do not depend on these ancillary processes.

In the limit of zero binding time, the ratio of the isomeric complexes formed is entirely determined by the ratio of their binding rate constants $k_{on,1}$ and $k_{on,2}$. If the binding reaction is carried out under the same conditions of temperature and pH as the dissociation reactions, these binding rate constants are related to the dissociation and interconversion rate constants of the complexes through a thermodynamic cycle:

$$\frac{k_{on,1}}{k_{off,1}}\frac{k_{12}}{k_{21}}\frac{k_{off,2}}{k_{on,2}} = K_{M\rightleftharpoons MP1}K_{MP1\rightleftharpoons MP2}K_{MP2\rightleftharpoons M} = 1 \qquad (3)$$

Consequently, the molar fraction of complex in the form $\{MP^*\}_1$ extrapolated to zero binding time can be expressed as

$$X_{\{MP^*\}_1}(0) = \frac{k_{off,1}k_{21}}{k_{off,1}k_{21} + k_{12}k_{off,2}} \qquad (4)$$

Because the magnitude of the observed fast dissociation phase is related to the fraction of $\{MP^*\}_1$ through Eq. 18 (Table 1), measurement of the magnitude of fast dissociation phase in the limit of zero binding time, F^o_0, provides additional information about the values of the microscopic rate constants of the MHC-peptide system.

We can calculate the F^o_0 values that would be observed for the candidate systems described by Schemes 1–5, using the rate constants provided. Of the five candidates discussed, Schemes 2, 4, and 5 are not consistent with the observed value $F^o_0 = 0.48$ for the binding variation data in Fig. 5. In terms of the "kinetic space" of MHC-peptide systems shown in Fig. 4, our measurement of F^o_0 restricts the range of possible candidates to the one-dimensional slice indicated by the dotted line.

TABLE 1 Relationships between the observed and microscopic kinetic parameters of a two-complex MHC-peptide system

$$k^o_{fast} = \frac{\Sigma k + (\Sigma k^2 - 4\Pi k)^{1/2}}{2} \qquad (16)$$

$$k^o_{slow} = \frac{\Sigma k - (\Sigma k^2 - 4\Pi k)^{1/2}}{2} \qquad (17)$$

$$F^o = \frac{(k_{off,1} - k_{off,2})X_{\{MP^*\}_1} + (k_{off,2} - k^o_{slow})}{k^o_{fast} - k^o_{slow}} \qquad (18)$$

$$S^o = \frac{(k_{off,1} - k_{off,2})X_{\{MP^*\}_2} + (k^o_{fast} - k_{off,1})}{k^o_{fast} - k^o_{slow}} \qquad (19)$$

with sum and product terms:

$$\Sigma k = k^o_{fast} + k^o_{slow} = k_{off,1} + k_{12} + k_{21} + k_{off,2} \qquad (20)$$

$$\Pi k = k^o_{fast}\,k^o_{slow} = k_{off,1}k_{21} + k_{off,1}k_{off,2} + k_{12}k_{off,2} \qquad (21)$$

Solving the equations in Table 1 for the parallel and sequential mechanisms gives general expressions for the limits of the microscopic parameters that are consistent with MHC-peptide dissociation experiments; these are shown in Table 2. Systems involving interconversion as well as direct dissociation of both complexes are characterized by values falling between the two extremes.

Like the magnitude of the fast dissociation phase at zero binding time, the value of F^o after infinite binding time is determined entirely by the system's microscopic interconversion and dissociation rate constants. In the limit of infinite binding time, the two isomeric MHC-peptide complexes are in equilibrium with each other; hence their populations are in the ratio of k_{12}/k_{21}, and the fraction of complex in the form $\{MP^*\}_1$ is

$$X_{\{MP^*\}_1}(\text{eq}) = \frac{k_{12}}{k_{12} + k_{21}} \tag{5}$$

The magnitude of the fast dissociation phase after binding to equilibrium is related to this fraction of $\{MP^*\}_1$ and is therefore also characteristic of the MHC-peptide system.

Interestingly, the magnitudes of the fast and slow exponential phases at zero and infinite binding time are related to one another in a fairly simple way. It can be shown that the kinetic equations in Table 1 lead to the relationship

$$\left(\frac{S^o}{F^o}\right)_{\text{eq}} = \frac{k^o_{\text{fast}}}{k^o_{\text{slow}}}\left(\frac{S^o}{F^o}\right)_0 \tag{6}$$

where S^o is the normalized magnitude of the slow phase. Because of this, it is useful to determine the value of F^o at both zero and infinite time as a check on the two-complex model. In a sigmoidal plot of slow/fast phase versus binding time, the extrapolated values at zero and infinity should be in the same ratio as the slow and fast observed dissociation rate constants.

Another useful feature of the S^o/F^o curve is illustrated in Fig. 5 *C*. At short incubation times, it can be shown that the curve approaches the line $y = y_0 + (1/2)y_0(k^o_{\text{fast}} - k^o_{\text{slow}})t$. This allows one to estimate the value of the S^o/F^o ratio—and therefore the value of F^o—at zero time from the value at a binding time t close to zero, using the formula

$$\left(\frac{S^o}{F^o}\right)_0 \cong \left(\frac{2}{2 + (k^o_{\text{fast}} - k^o_{\text{slow}})t}\right)\left(\frac{S^o}{F^o}\right)_t \tag{7}$$

It is important to note that the foregoing discussion is valid only if the binding conditions used to prepare the MHC-peptide complex are identical to the conditions of the dissociation reactions (except for peptide concentration). If binding and dissociation are performed under different conditions, the magnitude of the fast dissociation phase will depend on the microscopic rate constants under both sets of conditions, which greatly complicates the analysis of dissociation behavior for various binding times.

Even after dissociation is measured following a range of binding times, there is still a continuum of candidate systems that are consistent with the kinetic data, indicated by the dotted line in Fig. 4. To determine where our system lies along this line, we need measurements of the concentrations of the two complexes; the indirect readout provided by the magnitude of observed dissociation fast phase is not sufficient. Conventional kinetic measurements of MHC-peptide dissociation do not distinguish between different isomeric forms of the MHC-peptide complex, but other techniques may be used to detect and measure the two complexes. For example, ^{19}F NMR has been used to directly measure the relative populations of different complexes in several MHC-peptide systems (Schmitt et al., 1998a).

Consider the example of the peptide PCC, consisting of residues 89–104 of pigeon cytochrome *c*, bound to the class II MHC molecule I-E^k. Kinetic studies (Schmitt et al., 1998b) have shown that this system shows distinctly biphasic dissociation kinetics at pH 5.3 and 25°C, with observed rate constants of $k^o_{\text{fast}} = 1.70\ {}^{-0.29}_{+0.44}\ \text{h}^{-1}$ and $k^o_{\text{slow}} = 0.01397\ {}^{-0.00006}_{+0.00006}\ \text{h}^{-1}$. From the reported dissociation results following different binding times, we can estimate the ratio of the slow to the fast phase at zero binding time as $(F^o/S^o)_0 = 2.72\ {}^{-0.40}_{+0.47}$, corresponding to a fast phase at zero binding time of $F^o_0 = 0.27\ {}^{-0.03}_{+0.03}$. Separate NMR measurements (Schmitt et al., 1998a) have shown that when the complexes are isolated at pH 7.0 and 25°C, the fraction of complex in the form $\{MP^*\}_1$ is $X_{\{MP^*\}1} = 0.5\ {}^{-0.045}_{+0.045}$, and the magnitude of the fast phase in a subsequent dissociation at pH 5.3 and 25°C is $F^o(X_1 = 0.5) = 0.141\ {}^{-0.013}_{+0.013}$. Using these values, Eq. 4, and the equations in Table 1, we calculate that the microscopic rate constants of this system are $k_{\text{off},1} = 0.50\ {}^{-0.15}_{+0.25}\ \text{h}^{-1}$; $k_{12} = 1.17\ {}^{-0.28}_{+0.40}\ \text{h}^{-1}$; $k_{21} = 0.043\ {}^{-0.027}_{+0.068}\ \text{h}^{-1}$; $k_{\text{off},2} = 0.0013\ {}^{-0.0013}_{+0.0072}\ \text{h}^{-1}$. Based on these calculated rate constants, the equilibrium fraction of $\{MP^*\}_1$ at pH 5.3 is $X_{\{MP^*\}1}(\text{eq}) = 0.036\ {}^{-0.026}_{+0.078}$; this is very different from the value (~0.5) measured at pH 7.0. This example shows that some of the microscopic parameters, namely k_{21} and $k_{\text{off},2}$, are difficult to determine precisely; nevertheless

TABLE 2 Limits on the microscopic parameters consistent with observed dissociation curves

Parameter	Parallel mechanism	Sequential mechanism
$k_{\text{off},1}$	k^o_{fast}	$F^o_0\,k^o_{\text{fast}} + S^o_0\,k^o_{\text{slow}}$
k_{12}	0	$\dfrac{F^o_0\,S^o_0(k^o_{\text{fast}} - k^o_{\text{slow}})^2}{F^o_0\,k^o_{\text{fast}} + S^o_0\,k^o_{\text{slow}}}$
k_{21}	0	$\dfrac{k^o_{\text{fast}}\,k^o_{\text{slow}}}{F^o_0\,k^o_{\text{fast}} + S^o_0\,k^o_{\text{slow}}}$
$k_{\text{off},2}$	k^o_{slow}	0
For a given dissociation curve:		
$X_{\{MP^*\}_1}$	F^o	$\dfrac{F^o k^o_{\text{fast}} + S^o k^o_{\text{slow}}}{F^o_0\,k^o_{\text{fast}} + S^o_0\,k^o_{\text{slow}}}$

the calculated ranges do provide useful information about the system.

Hidden biphasic kinetics

Observation of a biphasic dissociation curve proves that isomeric forms of the MHC-peptide complex are present, even though they may not be detected directly. The inverse of this statement is not true, however. That is, the absence of an observed fast dissociation phase does not rule out the presence of multiple complexes. Indeed, if the dynamics of the MHC-peptide complexes are dominated by interconversion rather than dissociation, it can be virtually impossible to observe a biphasic dissociation curve, even though two different complexes are initially present.

For complexes prepared under the same conditions as the dissociation measurement, the maximum magnitude of observable fast phase is F_0^o, as can be seen in Fig. 5. From Eq. 18, we can derive an upper limit for F_0^o in terms of the interconversion rate of the complexes. For a relative interconversion rate of

$$k_i = \frac{(k_{12} + k_{21})}{(k_{off,1} + k_{off,2})} \tag{8}$$

the value of F_0^o cannot be greater than $1/(1 + k_i)$, and generally will be less than this, especially if the complex $\{MP^*\}_2$ has a significant dissociation rate. For example, if two MHC-peptide complexes have dissociation rate constants of 0.09 h^{-1} and 0.01 h^{-1} and interconversion rate constants of 6 h^{-1} and 4 h^{-1} (Scheme 5), then $k_i = 100$, and so F_0^o must be less than 0.01.

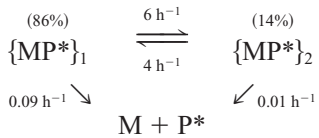

Scheme 6

Simulation of this system shows that the observed dissociation rate constants are 10.1 h^{-1} and 0.042 h^{-1}, but the value of F_0^o is only 0.0037 (Fig. 6, *circles*). This fast phase, with magnitude less than 0.4%, is impossible to detect using current methods.

Can systems with such rapid interconversion rates be physiologically relevant? In the example described above, the two complexes have characteristic lifetimes with respect to dissociation ($\tau_{off} = 1/k_{off}$) of 11 h and 100 h. By comparison, their lifetimes with respect to interconversion are 10 min and 15 min. Although the interconversion reactions are much more rapid than dissociation, interconversion is still slow enough to keep the two complexes distinct from a physiological point of view, even though they are not kinetically resolvable. In a physiological context, the important time scale is the lifetime of the ternary MHC-peptide/TCR complex, which is on the order of seconds (Matsui et al., 1991, 1994).

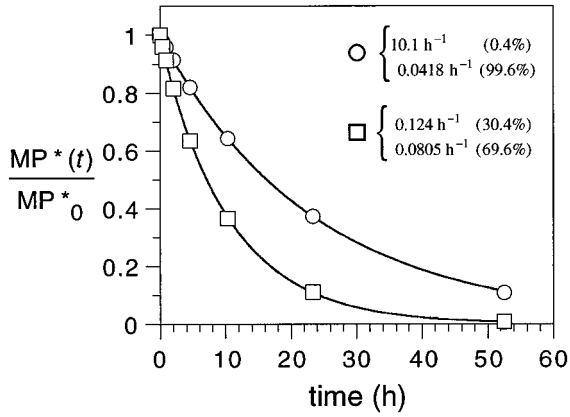

FIGURE 6 "Hidden" biphasic kinetics in MHC-peptide dissociation reactions: dissociation curves for the systems described by Schemes 6 (○) and 7 (□), after a very short binding incubation to maximize the amount of fast phase observed. The solid lines are single-exponential curve fits to the data.

Significantly, the magnitude of a fast dissociation phase may be undetectably small, even though the system initially contains a large fraction of $\{MP^*\}_1$. In the example shown in Scheme 6, the fraction of complex $\{MP^*\}_1$ present after a very short binding incubation is 85.7%; nevertheless, only a 0.4% fast phase is observed. The relatively fast interconversion renders the fast-dissociating complex "kinetically invisible" in dissociation experiments.

Another way in which a fast-dissociating MHC-peptide complex can evade kinetic detection is to have similar rate constants for the observed fast and slow dissociation phases. If the rate of interconversion is comparable to the rate of dissociation and the equilibrium constant between the two complexes favors the faster-dissociating $\{MP^*\}_1$, then the two observed rate constants can be very similar. Consider the system shown in Scheme 7:

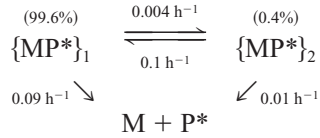

Scheme 7

Here the microscopic dissociation rate constants are the same as in Scheme 6, but the relative rate of interconversion, k_i, is only (0.004 h^{-1} + 0.1 h^{-1})/(0.09 h^{-1} + 0.01 h^{-1}) = 1.04. Even though the maximum magnitude of the fast dissociation phase for this system is a relatively high 30.4%, the observed rate constants of this system, 0.124 h^{-1} and 0.0805 h^{-1}, differ by only a factor of 1.5 (Fig. 6, *squares*). A double-exponential dissociation curve with such similar rate constants is virtually impossible to distinguish from a single-exponential curve, given the noise in current experiments (on the order of 1%). In general, two-complex systems like this one, with small equilibrium constants of interconversion ($K_i = k_{12}/k_{21}$), will have similar observed dissociation rate constants.

The examples of Schemes 6 and 7 illustrate that biphasic dissociation kinetics of a two-complex system can be difficult to resolve if either k_i or $1/K_i$ is greater than 1. Many two-complex systems may fall into one or both of the "unresolvable" categories illustrated by these schemes. This suggests the possibility that isomeric MHC-peptide complexes may be much more common than previously believed.

Although biphasic kinetics of an MHC-peptide system may be unresolvable under typical dissociation conditions, other conditions may produce more clearly biphasic behavior. MHC-peptide dissociation reactions are intrinsically relaxation processes, in which a sample prepared in the presence of labeled peptide is perturbed by removing unbound peptide and/or adding an excess of unlabeled competitor peptide. But other conditions, such as temperature and pH, can also be changed when dissociation is initiated. For example, a bound MHC-peptide complex may be stored at a low temperature (4°C) and then warmed to carry out a dissociation experiment at 25°C or 37°C. Alternatively, samples may be prepared at pH 5.3 for dissociations carried out at pH 7.0.

As discussed earlier, if the MHC-peptide complex is prepared under the same conditions as the dissociation reaction, the maximum magnitude of the dissociation fast phase is observed in the limit of zero binding time; this is also shown in Fig. 7 *A*. However, if the conditions are not the same, it may be possible to prepare the system such that the initial fraction of fast-dissociating $\{MP^*\}_1$—and hence the observed fast dissociation phase—is enhanced. This enhancement may permit the resolution of biphasic behavior for some systems. Fig. 7 *A* also shows that an interesting situation can result when the complex is prepared so that the initial fraction of $\{MP^*\}_1$ is very small. If the amount of $\{MP^*\}_1$ is small enough, the magnitude of observed fast dissociation can be zero or even negative! Such a dissociation appears to have a "lag period" at early time points (Fig. 7 *B*).

Another useful perturbation of the MHC-peptide system involves the addition of other chemical species to the reaction system. Dimethyl sulfoxide has been demonstrated to enhance peptide release from MHC (Schmitt et al., 1998a), as has the peptide dynorphin A (1–13) (de Kroon and McConnell, 1993; Schmitt, 1999). The chaperone molecule DM also catalyzes peptide release from MHC (Denzin and Cresswell, 1995). These substances appear to act disproportionately on the fast-dissociating isomer of the MHC-peptide complex, and as such may provide an aid in resolving two-complex dissociation kinetics.

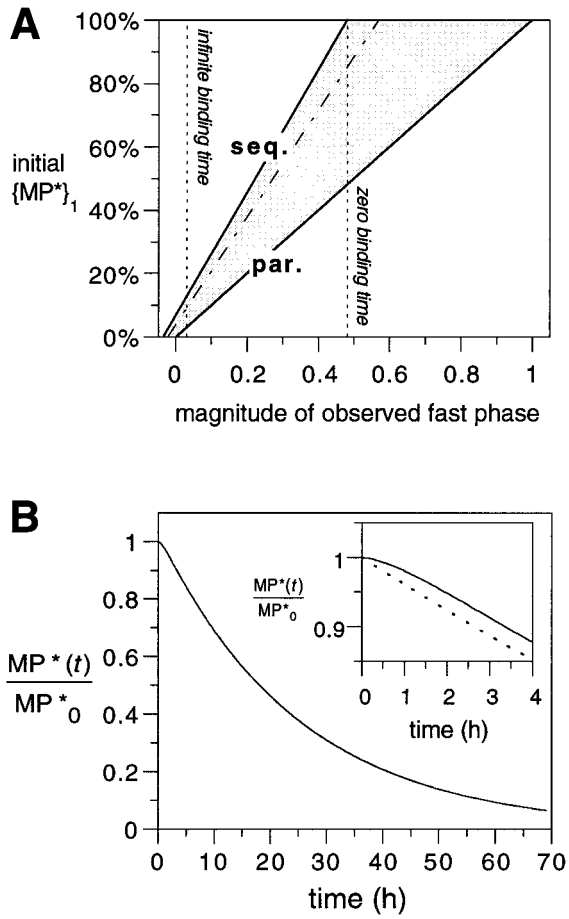

FIGURE 7 The magnitude of the observed dissociation fast phase generally does not reflect the initial amount of fast-dissociating complex. (*A*) The relationship between the magnitude of the observed fast phase, F^o, and the initial fraction of the fast-dissociating complex $\{MP^*\}_1$ is linear and depends on the interconversion and dissociation rates of the two complexes. For a given set of observed dissociations, consistent mechanisms span the range from parallel (e.g., Scheme 1), indicated by the heavy line labeled **par**, to sequential (e.g., Scheme 3), indicated by line **seq**. A dashed line (— - —) corresponds to the actual mechanism used for the simulation of Figs. 2 and 4. The observed fast dissociation phases in the limits of zero and infinite binding time are indicated by the vertical dotted lines. (*B*) A dissociation curve with a negative fast phase. Shown is a simulated dissociation curve for the two-complex system described in Scheme 3, starting from an initial population of 0.8% $\{MP^*\}_1$ and 99.2% $\{MP^*\}_2$; for this curve, $F^o = -0.034$. *Inset*: The early portion of the dissociation curve deviates from a single-exponential curve (*dotted line*).

CONCLUSIONS

Technical obstacles to measuring MHC-peptide reaction kinetics have largely been overcome (Witt and McConnell, 1993), but it is clear that such studies by themselves provide limited information about the isomers' dynamics. Although existing kinetic measurements cannot provide complete information about the reactions between MHC and peptides, the application of different techniques for characterizing MHC-peptide complexes and kinetics can help to focus the picture of these interactions.

This analysis also offers the prospect of resolving the mechanistic effects observed in changes in temperature (Witt and McConnell, 1994), pH (Witt and McConnell, 1991; Boniface et al., 1993; Schmitt et al., 1998b), and peptide sequence (Dornmair et al., 1991; Beeson et al., 1996; Liang et al., 1996; Schmitt et al., 1998b), which may be relevant to the biological function of these multiple-isomer MHC-peptide complexes. A further objective of this

work is to extend our analysis to the binding reactions of peptides to MHC molecules. These reactions, which have obvious importance in the understanding of MHC-peptide interactions, have been demonstrated to show complicated kinetics (Tampé and McConnell, 1991; Witt and McConnell, 1991, 1992; de Kroon and McConnell, 1993; Mason and McConnell, 1994; Rabinowitz et al., 1998; Natarajan et al., 1999) and are not merely the "reverse" of the dissociation reactions.

Finally, we hope to use this work to guide single-molecule fluorescence studies of MHC-peptide systems. Structural differences between isomeric complexes may influence environment-sensitive fluorescent labels. Any difference in fluorescence between complexes could be exploited in single-molecule studies, for which the amount of fluorescence would provide a direct measure of the state of the bound peptide. Intensity correlation functions may also permit the determination of isomerization rates (Wennman et al., 1997). Single molecule techniques are discussed in a recent issue of *Science* (Gimzewski and Joachim, 1999; Mehta et al., 1999; Moerner and Orrit, 1999; Weiss, 1999).

APPENDIX: ANALYTICAL SOLUTION OF THE RATE EQUATIONS

In general, for a system of N chemical species interacting by first-order ($A \rightarrow B$) reactions, the time-dependent concentrations of the species can be described by an $(N - 1)$-exponential curve plus a constant equilibrium value (Moore and Pearson, 1981). For the irreversible dissociation of isomeric MHC-peptide complexes shown in Fig. 1 *B*, $N = 3$ (complexes $\{MP^*\}_1$ and $\{MP^*\}_2$, and the dissociated state), and the equilibrium concentrations of the complexes are zero. Hence the total concentration of the two complexes during an irreversible dissociation reaction can be described by a biexponential curve.

Expressions for the macroscopic rate constants k^o_{fast} and k^o_{slow} of this biexponential curve can be found by integrating the rate equations for the reactions shown in Fig. 1 *B*. The concentrations of the three MHC species are described by the differential equations

$$\frac{d[\{MP^*\}_1]}{dt} = -(k_{off,1} + k_{12})[\{MP^*\}_1] + k_{21}[\{MP^*\}_2] \quad (9)$$

$$\frac{d[\{MP^*\}_2]}{dt} = k_{12}[\{MP^*\}_1] - (k_{21} + k_{off,2})[\{MP^*\}_2] \quad (10)$$

$$\frac{d[M]}{dt} = k_{off,1}[\{MP^*\}_1] + k_{off,2}[\{MP^*\}_2] \quad (11)$$

Solving this system of differential equations gives the expressions for the macroscopic rate constants k^o_{fast} and k^o_{slow} shown in Table 1, as well as expressions for the coefficients F^o and S^o.

The observed magnitudes of fast and slow phase, F^o and S^o, correspond to the sums of the two complexes' fast and slow coefficients. Expressions for these magnitudes can also be derived by examining the total dissociation rate of the complexes in terms of the concentrations and rate constants involved. From the mechanism in Fig. 1 *B*, we can express the initial rate of the dissociation reaction of an MHC-peptide system as

$$-\frac{d[\{MP^*\}]}{dt}(0) = [\{MP^*\}_1]k_{off,1} + [\{MP^*\}_2]k_{off,2} \quad (12)$$

Normalized with respect to the total initial concentration of the MHC-peptide complex, this becomes

$$-\frac{dMP^*}{dt}(0) = X_{\{MP^*\}_1}k_{off,1} + X_{\{MP^*\}_2}k_{off,2} \quad (13)$$

where $X_{\{MP^*\}1}$ and $X_{\{MP^*\}2}$ are the initial fractions of the two complexes.

A similar rate equation can be written based on the empirical biphasic concentration curve (Eq. 2) that is fit to the dissociation data. Differentiating this (already normalized) function with respect to time gives the initial dissociation rate as

$$-\frac{dMP^*}{dt}(0) = F^o k^o_{fast} + S^o k^o_{slow} \quad (14)$$

Combining Eqs. 13 and 14 gives the relation

$$X_{\{MP^*\}_1}k_{off,1} + X_{\{MP^*\}_2}k_{off,2} = F^o k^o_{fast} + S^o k^o_{slow} \quad (15)$$

Given that $X_{\{MP^*\}1} + X_{\{MP^*\}2} = 1$ and $F^o + S^o = 1$, Eq. 15 can be rearranged to give the expressions for F^o and S^o shown in Table 1.

The authors thank Lutz Schmitt for many helpful discussions.

This material is based upon work supported under a National Science Foundation Graduate Fellowship. This work was also supported by grant 5R37 AI13587-23 from the National Institutes of Health.

REFERENCES

Abbas, A. K., A. H. Lichtman, and J. S. Pober. 1994. Cellular and Molecular Immunology. W. B. Saunders Company, Philadelphia.

Beeson, C., T. G. Anderson, C. Lee, and H. M. McConnell. 1996. Isomeric complexes of peptides with class II proteins of the major histocompatibility complex. *J. Am. Chem. Soc.* 118:977–980.

Beeson, C., and H. M. McConnell. 1994. Kinetic intermediates in the reactions between peptides and proteins of major histocompatibility class II. *Proc. Natl. Acad. Sci. USA.* 91:8842–8845.

Boniface, J. J., N. L. Allbritton, P. A. Reay, R. M. Kantor, L. Stryer, and M. M. Davis. 1993. pH affects both the mechanism and the specificity of peptide binding to a class II major histocompatibility complex molecule. *Biochemistry.* 32:11761–11768.

Boniface, J. J., D. S. Lyons, D. A. Wettstein, N. L. Allbritton, and M. M. Davis. 1996. Evidence for a conformational change in a class II major histocompatibility complex molecule occurring in the same pH range where antigen binding is enhanced. *J. Exp. Med.* 183:119–126.

Brown, J. H., T. S. Jardetzky, J. C. Gorga, L. J. Stern, R. G. Urban, J. L. Strominger, and D. C. Wiley. 1993. Three-dimensional structure of the human class II histocompatibility antigen HLA-DR1. *Nature.* 364: 33–39.

Dadaglio, G., C. A. Nelson, M. B. Deck, S. J. Petzold, and E. R. Unanue. 1997. Characterization and quantitation of peptide-MHC complexes produced from hen egg lysozyme using a monoclonal antibody. *Immunity.* 6:727–738.

Davis, M. M. 1990. T cell receptor gene diversity and selection. *Annu. Rev. Biochem.* 59:475–496.

Davis, M. M., and P. J. Bjorkman. 1988. T-cell antigen receptor genes and T-cell recognition. *Nature.* 334:395–402.

de Kroon, A. I. P. M., and H. M. McConnell. 1993. Enhancement of peptide antigen presentation by a second peptide. *Proc. Natl. Acad. Sci.* 90:8797–8801.

de Kroon, A. I. P. M., and H. M. McConnell. 1994. Kinetics and specificity of peptide-MHC class II complex displacement reactions. *J. Immunol.* 152:609–619.

Denzin, L. K., and P. Cresswell. 1995. HLA-DM induces CLIP dissociation from MHC class II $\alpha\beta$ dimers and facilitates peptide loading. *Cell.* 82:155–165.

Dornmair, K., B. R. Clark, and H. M. McConnell. 1991. Binding of truncated peptides to the MHC molecule IA^d. *FEBS Lett.* 294:244–246.

Dornmair, K., B. Rothenhaüsler, and H. M. McConnell. 1989. Structural intermediates in the reactions of antigenic peptides with MHC molecules. *Cold Spring Harb. Symp. Quant. Biol.* 54:409–416.

Fremont, D. H., W. A. Hendrickson, P. Marrack, and J. Kappler. 1996. Structures of an MHC class II molecule with covalently bound single peptides. *Science.* 272:1001–1004.

Fremont, D. H., D. Monnaie, C. A. Nelson, W. A. Hendrickson, and E. R. Unanue. 1998. Crystal structure of $I\text{-}A^k$ in complex with a dominant epitope of lysozyme. *Immunity.* 8:305–317.

Garboczi, D. N., P. Ghosh, U. Utz, Q. R. Fan, W. E. Biddison, and D. C. Wiley. 1996. Structure of the complex between human T-cell receptor, viral peptide and HLA-A2. *Nature.* 384:134–141.

Garcia, K. C., M. Degano, R. L. Stanfield, A. Brunmark, M. R. Jackson, P. A. Peterson, L. Teyton, and I. A. Wilson. 1996. An $\alpha\beta$ T cell receptor structure at 2.5 Å and its orientation in the TCR-MHC complex. *Science.* 274:209–219.

Gimzewski, J. K., and C. Joachim. 1999. Nanoscale science of single molecules using local probes. *Science.* 283:1683–1688.

Jardetzky, T. 1997. Not just another Fab: the crystal structure of a TcR-MHC-peptide complex. *Structure.* 5:159–163.

Jardetzky, T. S., J. H. Brown, J. C. Gorga, L. J. Stern, R. G. Urban, J. L. Strominger, and D. C. Wiley. 1996. Crystallographic analysis of endogenous peptides associated with HLA-DR1 suggests a common, polyproline II-like conformation for bound peptides. *Proc. Natl. Acad. Sci.* 93:734–738.

Jensen, P. E. 1992. Long-lived complexes between peptide and class II major histocompatibility complex are formed at low pH with no requirement for pH neutralization. *J. Exp. Med.* 176:793–798.

Liang, M. N., C. Beeson, K. Mason, and H. M. McConnell. 1995. Kinetics of the reactions between the invariant chain (85–99) peptide and proteins of the murine class II MHC. *Int. Immunol.* 7:1397–1404.

Liang, M. N., C. Lee, Y. Xia, and H. M. McConnell. 1996. Molecular modeling and design of invariant chain peptides with altered dissociation kinetics from class II MHC. *Biochemistry.* 35:14734–14742.

Mason, K., and H. M. McConnell. 1994. Short-lived complexes between myelin basic protein peptides and IA^k. *Proc. Natl. Acad. Sci.* 91: 12463–12466.

Matsui, K., J. J. Boniface, P. A. Reay, H. Schild, B. F. d. S. Groth, and M. M. Davis. 1991. Low affinity interaction of peptide-MHC complexes with T cell receptors. *Science.* 254:1788–1791.

Matsui, K., J. J. Boniface, P. Steffner, P. A. Reay, and M. M. Davis. 1994. Kinetics of T-cell receptor binding to peptide/I-Ek complexes: correlation of the dissociation rate with T-cell responsiveness. *Proc. Natl. Acad. Sci.* 91:12862–12866.

Mehta, A. D., M. Rief, J. A. Spudich, D. A. Smith, and R. M. Simmons. 1999. Single-molecule biomechanics with optical methods. *Science.* 283:1689–1695.

Moerner, W. E., and M. Orrit. 1999. Illuminating single molecules in condensed matter. *Science.* 283:1670–1676.

Moore, J. W., and R. G. Pearson. 1981. Kinetics and Mechanism. John Wiley and Sons, New York.

Natarajan, S. K., M. Assadi, and S. Sadegh-Nasseri. 1999. Stable peptide binding to MHC class II molecule is rapid and is determined by a receptive conformation shaped by prior association with low affinity peptides. *J. Immunol.* 162:4030–4036.

Rabinowitz, J. D., M. N. Liang, K. Tate, C. Lee, C. Beeson, and H. M. McConnell. 1997. Specific T cell recognition of kinetic isomers in the binding of peptide to class II major histocompatibility complex. *Proc. Natl. Acad. Sci.* 94:8702–8707.

Rabinowitz, J. D., M. Vrljic, P. M. Kasson, M. N. Liang, R. Busch, J. J. Boniface, M. M. Davis, and H. M. McConnell. 1998. Formation of a highly peptide-receptive state of class II MHC. *Immunity.* 9:699–709.

Runnels, H. A., J. C. Moore, and P. E. Jensen. 1996. A structural transition in class II major histocompatibility complex proteins at mildly acidic pH. *J. Exp. Med.* 183:127–136.

Sadegh-Nasseri, S., and H. M. McConnell. 1989. A kinetic intermediate in the reaction of an antigenic peptide and $I\text{-}E^k$. *Nature.* 338:274–276.

Sadegh-Nasseri, S., L. J. Stern, D. C. Wiley, and R. N. Germain. 1994. MHC class II function preserved by low-affinity peptide interactions preceding stable binding. *Nature.* 370:647–650.

Schmitt, L. 1999. Catalysis of peptide dissociation from class II MHC-peptide complexes. *Proc. Natl. Acad. Sci.* 96:6581–6586.

Schmitt, L., J. J. Boniface, M. M. Davis, and H. M. McConnell. 1998a. Conformational isomers of a class II MHC-peptide complex in solution. *J. Mol. Biol.* 286:2409–2420.

Schmitt, L., J. J. Boniface, M. M. Davis, and H. M. McConnell. 1998b. Kinetic isomers of a class II MHC-peptide complex. *Biochemistry.* 37:17371–17380.

Scott, C. A., P. A. Peterson, L. Teyton, and I. A. Wilson. 1998. Crystal structures of two $I\text{-}A^d$-peptide complexes reveal that high affinity can be achieved without large anchor residues. *Immunity.* 8:319–329.

Steinfeld, J. I., J. S. Francisco, and W. L. Hase. 1989. Chemical Kinetics and Dynamics. Prentice-Hall, Englewood Cliffs, NJ.

Tampé, R., and H. McConnell. 1991. Kinetics of antigenic peptide binding to the class II major histocompatibility molecule I-Ad. *Proc. Natl. Acad. Sci.* 88:4661–4665.

Tulp, A., D. Verwoerd, B. Dobberstein, H. L. Ploegh, and J. Pieters. 1994. Isolation and characterization of the intracellular MHC class II compartment. *Nature.* 369:120–126.

Viner, N. J., C. A. Nelson, B. Deck, and E. R. Unanue. 1996. Complexes generated by the binding of free peptides to class II MHC molecules are antigenically diverse compared with those generated by intracellular processing. *J. Immunol.* 156:2365–2368.

Weiss, S. 1999. Fluorescence spectroscopy of single biomolecules. *Science.* 283:1676–1683.

Wennman, S., L. Edman, and R. Rigler. 1997. Conformational fluctuations in single DNA molecules. *Proc. Natl. Acad. Sci. USA.* 94:10641–10646.

Witt, S. N., and H. M. McConnell. 1991. A first-order reaction controls the binding of antigenic peptides to major histocompatibility complex class II molecules. *Proc. Natl. Acad. Sci.* 88:8164–8168.

Witt, S. N., and H. M. McConnell. 1992. Antigenic peptide binding to the mouse major histocompatibility complex class II protein $I\text{-}E^k$. Peptide stabilization of the quaternary structure of $I\text{-}E^k$. *J. Am. Chem. Soc.* 114:3506–3511.

Witt, S. N., and H. M. McConnell. 1993. The kinetics of peptide reactions with class II major histocompatibility complex membrane proteins. *Acc. Chem. Res.* 26:442–448.

Witt, S. N., and H. M. McConnell. 1994. Formation and dissociation of short-lived class II MHC-peptide complexes. *Biochemistry.* 33: 1861–1868.